

Elastic Properties of New Solid State Electrolyte Material $\text{Li}_{10}\text{GeP}_2\text{S}_{12}$: A Study from First-Principles Calculations

Z. Q. Wang, M. S. Wu, G. Liu, X. L. Lei, B. Xu, C. Y. Ouyang*

Department of Physics, Jiangxi Normal University, Nanchang, 330022, P. R. China

*E-mail: cyouyang@jxnu.edu.cn

Received: 23 October 2013 / Accepted: 19 November 2013 / Published: 8 December 2013

Elastic properties of a new ultrafast lithium ion conductor $\text{Li}_{10}\text{GeP}_2\text{S}_{12}$ were studied from first-principles calculations. The six independent elastic constants (C_{11} , C_{12} , C_{13} , C_{33} , C_{44} , and C_{66}) are obtained and the results satisfy the Born's criteria of lattice stability. The bulk modulus B , shear modulus G , Young's modulus E , elastic modulus λ and Poisson's ratio ν were calculated to be 30.36 GPa, 14.35 GPa, 37.19 GPa, 20.80 GPa and 0.296, respectively. The B/G ratio is derived to be 2.12, implying that the $\text{Li}_{10}\text{GeP}_2\text{S}_{12}$ is ductile according to Pugh's criterion. The Van der Waals interactions are important in calculation of the elastic properties.

Keywords: Lithium ion batteries; $\text{Li}_{10}\text{GeP}_2\text{S}_{12}$; Elastic properties; First principles calculations.

1. INTRODUCTION

Lithium ion batteries play more and more important role in modern life. They have already widely used in consumer electronics, and will have vast applications as power supplier in electric vehicles (EV) and as energy storage medium for wind and solar energy. The great demand for batteries with high power and energy densities promotes the need for advanced lithium ion batteries materials and technologies [1, 2]. Along the way to the commercialization of EV, the safety problem of lithium ion batteries must be solved in advance before it can be widely accepted by common consumers. To solve the safety problem, one strategy is to develop all solid state lithium ion batteries that use the solid-state electrolytes (SSE), which have many advantages such as good stability, high safety, and scalability when compared to their liquid counterparts [3, 4]. Now, SSEs are promising to replace current flammable organic liquid electrolytes. However, the ionic conductivity in most SSEs does not reach competitive levels [4, 5].

The thio-LISICON SSEs composed of $\text{Li}_2\text{S-P}_2\text{S}_5$ systems are studied extensively in the past two decades [6-9]. Among the thio-LISICON group, $\text{Li}_7\text{P}_3\text{S}_{11}$ and $\text{Li}_4\text{P}_2\text{S}_7$ are two typical examples and are most widely studied [10, 11]. Recently, a new type of ultrafast lithium ion conductor $\text{Li}_{10}\text{GeP}_2\text{S}_{12}$ (LGPS) was synthesized by Kamaya et al. [12] and soon attracted considerable attention of both the academic and the industrial fields. LGPS has achieved very high room temperature Li ion conductivity of 12 mS/cm, which is even higher than that of the commercialized liquid electrolyte. As a promising SSE, the lithium ion diffusion mechanism [4], the phase and structural stability [13], and the electrochemical performances of LGPS [14-16] are studied by many researchers in recent two years. *Ab initio* and classical molecular dynamics are performed to simulate the lithium ion diffusion in LGPS, and it is found that lithium ion diffusion pathway is along the *c*-axis direction of the lattice. The lithium ion diffusion energy barrier (activation energy) is about 0.2 eV, with small variation when different methods are applied.

Although it is demonstrated that LGPS is applicable as a practical electrolyte for all solid state lithium ion batteries, the solid-solid interface between the SSE and the powder electrode material is still an important technological problem during the process of the battery assembly. Unlike the liquid electrolyte, the solid-solid contact could be very bad. This increases the interfacial resistance/impedance and thus results in very poor rate performance of the solid state battery system. Furthermore, the cycling performance of battery is also closely related with the character of the solid-solid interface. Generally speaking, it demonstrates good performance in terms of device fabrication, cycling performance and safety, if the electrolyte material is ductile. The mechanical properties (particularly the malleability and the ductility) of the SSE and the electrode materials have a great impact on the contact condition of electrolyte and electrode materials. In order to improve the solid-solid contact between the electrolyte and the electrode materials, it is necessary to improve the mechanical properties of the SSE.

However, the mechanical properties of LGPS remain unclear to the literature. Before wide application of the LGPS material in all solid state lithium battery system, it is very important to figure out these mechanical characteristics, which are of interest to both the academic and industrial researchers. In the present work, we studied the elastic properties of the LGPS from first principles calculations, together with other two thio-LISICON family members $\text{Li}_4\text{P}_2\text{S}_7$ and $\text{Li}_3\text{P}_7\text{S}_{11}$ for comparison. The six independent elastic constants, the bulk modulus *B*, shear modulus *G*, Young's modulus *E*, elastic modulus λ , and Poisson's ratio ν of the LGPS were calculated. Those data provide useful information for the reference of other experimental researchers.

2. COMPUTATIONAL DETAILS AND THEORETICAL BACKGROUNDS

Calculations are performed within the density-functional theory (DFT) and the plane-wave pseudopotential method, which are implemented in the Vienna *ab initio* simulation package (VASP) [17]. The core ion and valence electron interaction are described by the projector augmented wave (PAW) method and the exchange-correlation part is described with the Perdew-Burke-Ernzerhof (PBE) [18]. Energy cut off for the plane waves is chosen to be 500 eV. The Monkhorst-Pack [19]

scheme K-points sampling with $5 \times 5 \times 3$ k -points grid is used for the $8.72 \text{ \AA} \times 8.72 \text{ \AA} \times 12.63 \text{ \AA}$ unit cell of LGPS [12]. Similar accuracy is also applied for calculations of other materials in the present work. Since the structure of the LGPS is composed of GeS_4 and PS_4 tetrahedrons that are not connected with each other through sharing atoms or edges, the Van der Waals (VDW) interactions among these tetrahedrons could be important and therefore are taken into consideration in this study. Before we calculate the elastic parameters, the lattice parameters are optimized the atomic positions are fully relaxed until the final forces on all relaxed atoms are less than 0.05 eV \AA^{-1} .

Generally, the bulk modulus can be calculated through fitting the total energy calculated at different lattice constants to the Murnaghan equation of state [20, 21]. The elastic constants can be obtained by calculating the total energy as a function of the strains. For small strain applied on solids, the Hook's law is applicable and the elastic energy ΔE is a quadratic function of the strains

$$\Delta E = V \sum_{i,j=1}^6 \frac{1}{2} C_{ij} e_i e_j \quad (1)$$

Where C_{ij} are the elastic constants, V is the volume of the unit cell under equilibrium state. The e_i and e_j are the components of strain matrix. For a tetragonal crystal, there are six independent (non-zero) elastic constants, namely, C_{11} , C_{12} , C_{13} , C_{33} , C_{44} and C_{66} . The elastic constants matrix can be expressed in the following form:

$$C_{ij} = \begin{pmatrix} C_{11} & C_{12} & C_{13} & 0 & 0 & 0 \\ C_{12} & C_{11} & C_{13} & 0 & 0 & 0 \\ C_{13} & C_{13} & C_{33} & 0 & 0 & 0 \\ 0 & 0 & 0 & C_{44} & 0 & 0 \\ 0 & 0 & 0 & 0 & C_{44} & 0 \\ 0 & 0 & 0 & 0 & 0 & C_{66} \end{pmatrix} \quad (2)$$

The bulk modulus and shear modulus can be directly obtained from the six independent elastic constants:

$$B = \frac{2C_{11} + 2C_{12} + 4C_{13} + C_{33}}{9} \quad (3)$$

$$G = \frac{1}{15} (2C_{11} + C_{33} - C_{12} - 2C_{13}) + \frac{1}{5} (2C_{44} + C_{66}) \quad (4)$$

In order to calculate the six independent elastic constants, we calculated the total energy changes of the system upon six strains along different directions that are applied to the unit cell. In the present work, the six strains are chosen as: $(\delta, \delta, 0, 0, 0, 0)$, $(0, 0, 0, 0, 0, \delta)$, $(0, 0, \delta, 0, 0, 0)$, $(0, 0, 0, \delta, \delta, 0)$, $(\delta, \delta, \delta, 0, 0, 0)$ and $(0, \delta, \delta, 0, 0, 0)$. The elastic constants can be obtained through fitting Eq. 1. Then, the Young's modulus, elastic modulus and Poisson's ratio can be obtained by using the bulk modulus and shear modulus:

$$E = \frac{9BG}{3B + G} \quad (5)$$

$$\lambda = B - \frac{2}{3}G \quad (6)$$

$$\nu = \frac{3B - 2G}{2(3B + G)} \quad (7)$$

3. RESULTS AND DISCUSSION

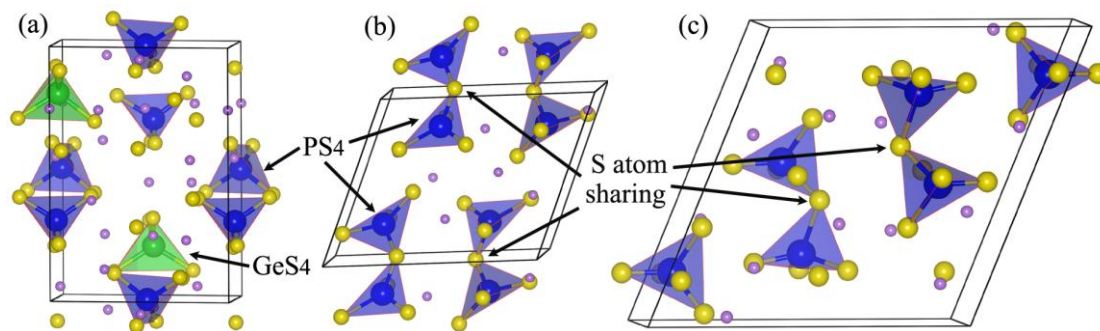


Figure 1. Schematic view of the atomic structures of LGPS (a), $\text{Li}_4\text{P}_2\text{S}_7$ (b), and $\text{Li}_7\text{P}_3\text{S}_{11}$ (c). The PS_4 and GeS_4 tetrahedrons and the S atom shared PS_4 tetrahedrons are marked with arrows.

The atomic structures of LGPS, $\text{Li}_4\text{P}_2\text{S}_7$, and $\text{Li}_7\text{P}_3\text{S}_{11}$ are schematically shown in Figure 1. The LGPS has a tetragonal unit cell, which consists of GeS_4 and PS_4 tetrahedrons, and Li atoms occupy the octahedral and tetrahedral sites [12]. The Li atoms are fully ionized into Li ions and Coulomb attraction force exists between Li ion and PS_4 (GeS_4) tetrahedrons, which binds them into solid structure.

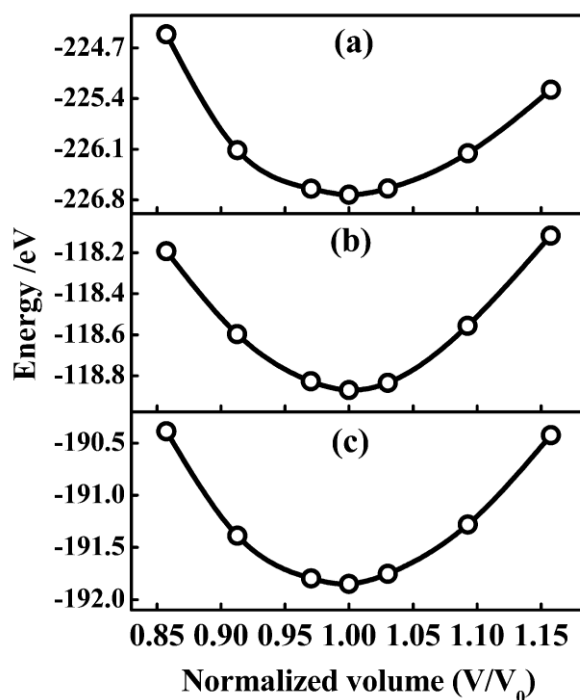


Figure 2. Evolution of the total energy as a function of the unit cell volume of LGPS (a), $\text{Li}_4\text{P}_2\text{S}_7$ (b) and $\text{Li}_7\text{P}_3\text{S}_{11}$ (c). The VDW energies are included.

The $\text{Li}_4\text{P}_2\text{S}_7$ has a triclinic unit cell [7, 8]. The backbone of $\text{Li}_4\text{P}_2\text{S}_7$ is composed of P_2S_7 dimers, which is formed by two neighbouring PS_4 tetrahedron combined together through sharing one

S atom. Like the structure of $\text{Li}_4\text{P}_2\text{S}_7$, the $\text{Li}_7\text{P}_3\text{S}_{11}$ also has a triclinic unit cell [7, 8], which is composed of Li_3PS_4 monomer and $\text{Li}_4\text{P}_2\text{S}_7$ dimer components. From this perspective, the backbones of $\text{Li}_7\text{P}_3\text{S}_{11}$ are composed of P_2S_7 dimers and PS_4 tetrahedrons with the 1:1 ratio.

Figure 2 gives the total energy variation as a function of the volume of the unit cell for LGPS, $\text{Li}_4\text{P}_2\text{S}_7$, and $\text{Li}_7\text{P}_3\text{S}_{11}$. The equilibrium lattice constant and the bulk modulus can be obtained by fitting these data to the Murnaghan equation of states. In order to test the influence of the VDW interaction to the mechanic properties, we also calculated the bulk moduli of the three compounds without taking into account the VDW for comparison.

Table 1. The bulk moduli (B in GPa) of LGPS, $\text{Li}_4\text{P}_2\text{S}_7$ and $\text{Li}_7\text{P}_3\text{S}_{11}$ with (VDW) and without (No-VDW) taking into consideration of the Van der Waals interactions in the total energy calculation.

LGPS		$\text{Li}_4\text{P}_2\text{S}_7$		$\text{Li}_7\text{P}_3\text{S}_{11}$	
VDW	No-VDW	VDW	No-VDW	VDW	No-VDW
29.74	20.43	18.30	15.65	24.00	22.99

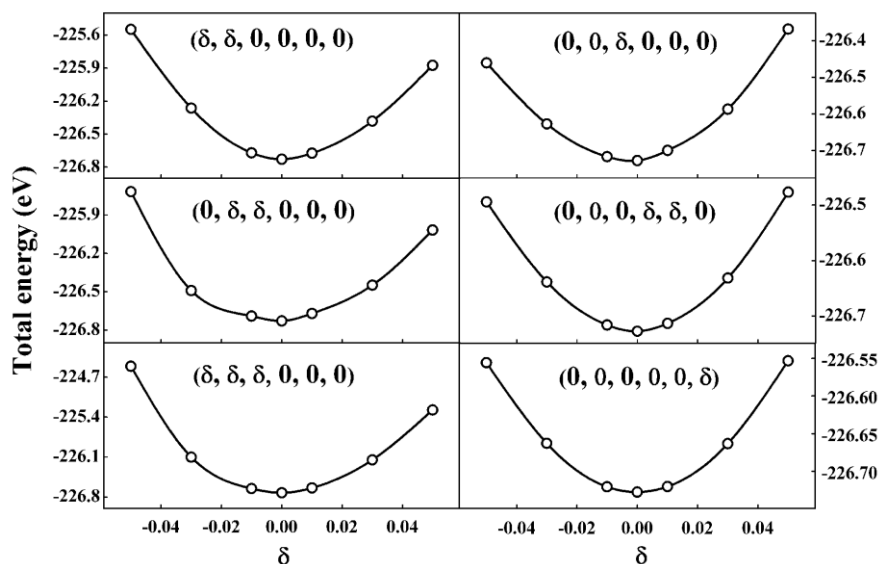


Figure 3. Strain energy of deformation as a function of deformation parameter for six different deformations in LGPS.

Table 1 gives the theoretically obtained bulk modulus of the LGPS together with the other two typical compounds of the thio-LISICON $\text{Li}_4\text{P}_2\text{S}_7$ and $\text{Li}_7\text{P}_3\text{S}_{11}$. The bulk modulus of LGPS is larger than the other two Thio-LISICON compounds. This makes the battery assembly process more difficult if we replace the $\text{Li}_4\text{P}_2\text{S}_7$ and $\text{Li}_7\text{P}_3\text{S}_{11}$ SSEs with LGPS. For example, it needs a higher pressure to make the contact between the electrode powder and the LGPS powder as compact as it is for $\text{Li}_4\text{P}_2\text{S}_7$ and $\text{Li}_7\text{P}_3\text{S}_{11}$. Interestingly, the higher bulk modulus of LGPS than the other two compounds is due to

the VDW interaction. The calculated bulk modulus of LGPS increased about 45.6% from 20.43 GPa to 29.74 GPa when the VDW interactions are included into the total energy calculation. On the contrary, the bulk moduli of the $\text{Li}_4\text{P}_2\text{S}_7$ and $\text{Li}_7\text{P}_3\text{S}_{11}$ are not very sensitive to the VDW interaction, although the VDW interaction enhanced the B values to some degree. Fig. 3 shows the change in total energies as a function of strain applied in six directions. Through fitting these energy changes and the applied strain data, we can calculate the six independent elastic constants of LGPS, as listed in Table 2.

Table 2. Calculated elastic constants (C_{ij} in GPa) of LGPS

C_{11}	C_{12}	C_{13}	C_{33}	C_{44}	C_{66}
36.03	35.88	21.32	44.15	17.21	24.79

To the best of our knowledge, there is no experimental or theoretical elastic constant data of LGPS are available in literature. We can't compare these theoretical elastic constants with others. According to Born's criteria of lattice stability, for a tetragonal crystal the elastic constants should satisfy the following criteria [22, 23]:

$$\begin{aligned} (C_{11} - C_{12}) > 0, (C_{11} + C_{33} - 2C_{13}) > 0 \\ C_{11} > 0, C_{33} > 0, C_{44} > 0, C_{66} > 0 \\ (2C_{11} + C_{33} + 2C_{12} + 4C_{13}) > 0 \end{aligned} \quad (8)$$

From the data in Tab. 2, it is obvious that the calculated elastic constants satisfy the elastic stability criteria, which shows that the LGPS lattice/structure is stable at the ground state. With the above elastic constant data given in Tab. 2, we can calculate the bulk modulus B, the shear modulus G, Young's modulus E, elastic modulus λ , and Poisson's ratio ν , and the results are listed in Table 3.

Table 3. Calculated Bulk modulus (B in GPa), Shear modulus (G in GPa), Young's modulus (E in GPa), elastic modulus (λ in GPa), Poisson's ratio (ν), and the B/G ratio of the LGPS.

B	G	E	λ	ν	B/G
30.36	14.35	37.19	20.80	0.30	2.12

As a potential SSE material, the ductility/brittleness performance is very important since the electrode/electrolyte interface contact is crucial for better electrical conductance. This requires the SSE material is able to change its shape without fracture. Generally, we can evaluate the ductility/brittleness nature of a solid material through Pugh's criterion on the value of B/G ratio [24]. High bulk modulus B indicates of strong binding strength of the bonds (forces) in the solid, while high shear modulus represents large resistance to plastic deformation. Therefore, low B/G ratio indicates brittleness while high B/G ratio represents ductility. According to Pugh's criterion, when the B/G ratio is larger than 1.75 the solid material can be regarded as ductile [25]. As for LGPS compound, the B/G ratio is 2.12, indicating that LGPS is ductile and fracture will not occur easily upon mechanical pressure when it is used as solid state electrolyte.

4. SUMMARY AND CONCLUSIONS

In summary, we have investigated the structural and elastic properties of LGPS and other two compounds of the thio-LISICON family $\text{Li}_3\text{P}_7\text{S}_{11}$ and $\text{Li}_4\text{P}_2\text{S}_7$, by first-principles calculations. The bulk modulus of LGPS is larger than that of the $\text{Li}_4\text{P}_2\text{S}_7$ and $\text{Li}_7\text{P}_3\text{S}_{11}$. This makes the battery assembly process more difficult if we replace the $\text{Li}_4\text{P}_2\text{S}_7$ and $\text{Li}_7\text{P}_3\text{S}_{11}$ SSEs with LGPS. Fortunately, the calculated B/G ratio shows that the LGPS is ductile, which is in favor of the mechanical processing of the LGPS materials as SSE in all solid state lithium ion batteries. Interestingly, our results also show that the VDW interaction is very important to the mechanical properties of LGPS. It increases the bulk modulus of LGPS by 45.6%.

References

1. J.B. Goodenough, Y. Kim, *Chem. Mater.* 22 (2010) 587-603.
2. A.S. Acrico, P. Bruce, B. Scrosati, J.M. Tarascon, W.V. Schalkwijk, *Nat. Mater.* 4 (2005) 366-377.
3. Y. F. Mo, S. P. Ong, G. Ceder, *Chem. Mater.* 24 (2012) 15-17.
4. S. Adams, R. P. Rao *J. Mater. Chem.* 22 (2012) 7687-7691.
5. W. Li, G.T. Wu, C.M. Araujo, R.H. Scheicher, A. Blomqvist, R. Ahuja, Z.T. Xiong, Y. P. Feng, P. Chen, *Energy Environ. Sci.* 14 (2012) 1596–1606.
6. R. Kanno, M. Murayama, *J. Electrochem. Soc.* 148 (2001) A742.
7. N. D. Lepley and N. A. W. Holzwarth, *J. Electrochem. Soc.* 159(5) (2012) A538-A547.
8. N.A.W. Holzwarth, N.D. Lepley, Y. A. Du, *J. Power Sources* 196 (2011) 6870–6876.
9. T. Ohtomo, F. Mizuno, A. Hayashi, K. Tadanaga, M. Tatsumisago, *J. Power Sources*, 146 (2005) 715-718.
10. M. Tatsumisago, A. Hayashi, *Solid State Ionics*, 225 (2012) 342-345.
11. T. Inada, T. Kobayashi, N. Sonoyama, A. Yamada, S. Kondo, M. Nagao, R. Kanno, *J. Power Sources*, 194 (2009) 1085-1088.
12. N. Kamaya, K. Homma, Y. Yamakawa, M. Hirayama, R. Kanno, M. Yonemura, T. Kamiyama, Y. Kato, S. Hama, K. Kawamoto, A. Mitsui *Nat. mater.* 10 (2011) 682-686.
13. S. P. Ong, Y. F. Mo, W. D. Richards, L. Miara, H. S. Lee and G. Ceder, *Energy Environ. Sci.* 6 (2013) 148-156.
14. J. Hassoun, R. Verrelli, P. Reale, S. Panero, G. Mariotto, S. Greenbaum, B. Scrosati, *J. Power Sources* 229 (2013) 117-122.
15. Y. M. Wang, Z. Q. Liu, X. L. Zhu, Y. F. Tang, F. Q. Huang, *J. Power Sources*, 224 (2013) 225-229.
16. Y. Kato, K. Kawamoto, R. Kanno, M. Hirayama, *Electrochem.* 80 (2012) 749-751.
17. G. Kresse, J. Furthmuller, *Phys. Rev. B* 54 (1996) 11169-11186.
18. G. Kresse, J. Joubert, *Phys. Rev. B* 59 (1999) 1758-1775.
19. H. J. Monkhorst, J. D. Pack *Phys. Rev. B* 13 (1976) 5188-5192.
20. F. D. Murnaghan, *Proc. Natl. Acad. Sci. U. S. A.* 30 (1944) 244-247.
21. C. L. Fu, K. M. Ho, *Phys. Rev. B* 28 (1983) 5480-5486.
22. O. Beckstein, J. E. Klepeis, G. L. W. Hart, O. Pankratov, *Phys. Rev. B* 63 (2001) 134112.
23. H. F. Dong, H. F. Liu, *Solid State Commun.* 167 (2013) 1–4.
24. L. Vitos, P. A. Korzhavyi, B. Johansson, *Phys. Rev. Lett.*, 88 (2002) 155501.
25. S. F. Pugh, *Philos. Mag.* 45 (1954) 823-843.